Robust Fault Detection and Isolation using Bond Graph for an Active-Passive Variable Serial Elastic Actuator

P.J. Cheng *u9014028@gmail.com*
Department of Mechanical Engineering
National Taiwan University
Taipei, 10617, Taiwan

H.P. Huang *hanpang@ntu.edu.tw*
Department of Mechanical Engineering
National Taiwan University
Taipei, 10617, Taiwan

Abstract

A robot is a complex machine, comprising mechanism, actuators, sensors, and electrical system. It is, therefore, hard to guarantee that all the components can always function normally. If one component fails, the robot might harm humans. In order to develop the active-passive variable serial elastic actuator (APVSEA) [1] that can detect the occurrence of any component fault, this paper uses bond graph to design a robust fault detection and isolation (RFDI) system. When the robot components malfunction, the RFDI system will execute suitable isolation strategies to guarantee human safety and use zero-gravity control (ZGC) to simultaneously compensate for the torque caused by gravity. Thus, the user can consistently interact with the robot easily and safely. From the experimental results, the RFDI system can filter out uncertain parameters and identify the failed component. In addition, the zero-gravity control can lessen potentially physical damage to humans.

Keywords: Serial Elastic Actuator, Bond Graph, Fault Detection and Isolation, Zero Gravity Control.

1. INTRODUCTION

A robot system has various sensors and mechanism to detect the states and transmit energy. If any component malfunctions, it may crash the control system or the transmission mechanism, which is dangerous for humans. Robot technology has already been applied to factories. However, applications, such as home care, office security, or simply the cooperation with humans, are yet the next stage of robot development. In all these applications with robots working around humans, guaranteeing human safety is the most important issue. Actuator is a key element of the robot system. It can comprise robot arm, robot leg, robot wheel or exoskeleton. Therefore, it is important for making sure each actuator is working normally.

Fault detection and isolation (FDI) procedures are the combination of the actual system and its theoretical behavior [2-3]. Based on knowing the actual system sufficiently, a quantitative FDI approach derives the system's dynamic behavior and uses it as the reference model in terms of analytical redundancy relationships (ARRs). There are two main steps in FDI processing: the first is substituting the system's signals into the ARR equations; the second is the decision-making procedure, which detects faults and isolates fail components. After the substitution, the value of an ARR equation is called a residual. In perfect ARR equations, the residuals are zeros, which means the following

1. The model describes the system completely.
2. No uncertainty is in the model.
3. The system's signals are noiseless.

4. The system functions normally.

A real-world system, however, does not comply with such strict definitions. Uncertainty in models or noises from the external environment will generate false alarms. To solve this problem, setting suitable thresholds is a common approach. A setting with constant thresholds is feasible for regular machine motions, such as those of machine tools. But an intelligent robot's actuator targets may vary. For example, the force or position input commands of the robot arm are different. Those will cause the residual value unlike. Consequently, the thresholds should adapt to the robot's assigned mission. Many studies tried to solve the system-dependent dynamic threshold problem [4-9]. Djeziri et al. [10] proposed an adaptive FDI scheme to adjust thresholds dynamically which considers the conditions of nominal parameters and uncertainties. Walid et al. [11-12] proposed an adaptive fuzzy FDI method to adjust thresholds. Although the adaptive FDI can adjust thresholds dynamically based on the system's uncertain parts, there is still a need for parameters tuning; a false alarm will still sound if those parameters are not set properly.

Another associated aspect in FDI is fault tolerance control (FTC) which strengthens FDI safety mechanisms [13-16]. When component failures occur, FTC can switch the control system to a suitable controller to keep human safe or avoid mechanism to break. In some scenarios, such as wearable robots, a complete system shutdown is dangerous for humans, because the robot's weight could be harmed on human body. Therefore, zero-gravity control (ZGC) has been used to compensate for the gravity torque due to robot's mechanism [17-21], so that the robot can be easily moved and meet the safety requirement.

The main aim of this paper is to design a robust fault detection and isolation (RFDI) system for the active-passive variables serial elastic actuator (APVSEA) [1]. The RFDI combines adaptive FDI, doubt index, and FTC. We use the quantitative approach of bond graph to design FDI, which relies on system's model information. In addition to adaptive FDI, the doubt index, which increases if an alarm occurs frequently, can monitor potential false alarms. Using the doubt index to cast doubts on the alarm in the decision procedure, the RFDI system can determine whether a fault occurs in the robot system without signaling false alarms. Finally, for FTC, we design a ZGC by exploiting the flexible property of APVSEA as an economic alternate to realize ZGC.

In the following sections, adaptive FDI, doubt index, ZGC, and FTC are presented. In Section II, the principles and properties of APVSEA are introduced and modeled using bond graph. We also discuss how broken components of APVSEA could harm humans. The RFDI is proposed in Section III, and its application to APVSEA is described in Section IV. The experimental results of the proposed system are presented in Section V, and followed by conclusion.

2. OPERATIONAL PRINCIPLE AND MODELING OF APVSEA

2.1 Operational Principle of APVSEA [1]

In order to understand the effect on the system when one of the system components is broken, we first introduce the APVSEA operational principle and construct the bond graph model. The APVSEA is designed to be an intrinsically safe actuator. As shown in Figure 1, it consists of two parts: a serial elastic actuator and a mechanism that can actively or passively change the system's stiffness. It is assembled mainly with four components: DC motors, a ball screw, a moving plant, and springs. The potentiometer behind the spring is used to measure the displacement of the spring, and three encoders are used to measure the angles of the motor and the output link.

As shown in Figure 2, motor 01 is aimed to rotate the output link of APVSEA: motor 01 drives the ball screw though timing belt 01, the ball screw shifts the plant horizontally, and finally, timing belt 02 rotates the output link. On the other hand, motor 02 is used to change the stiffness of the APVSEA. Since this paper is focused on FDI using bond graph, we will not discuss the operational principle of motor 02. The interested readers can refer to [1] for details.

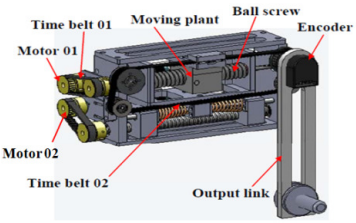

FIGURE 1: APVSEA 3D Diagram.

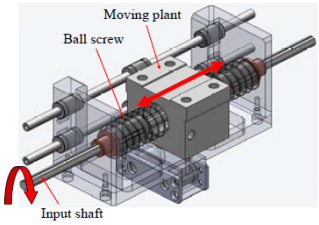

FIGURE 2: Moving Plant is Moved by Motor 01.

As an intrinsically safe mechanism, APVSEA can absorb external forces. If external forces are applied to the output link, the moving plant is driven by the external forces via timing belt 02, but the ball screw is not directly driven back by the moving plant. Instead, the moving plant slips on the input shaft, because external forces generate an axial force. Therefore, when the translation of the moving plant occurs, the springs of the APVSEA can absorb external forces by the connector, as shown in Figure 3 and Figure 4.

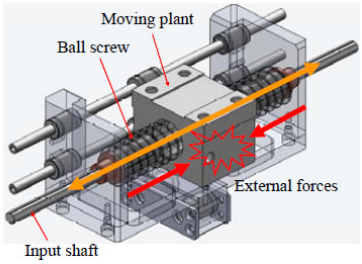

FIGURE 3: External Force Generates Axial Slipping Motion.

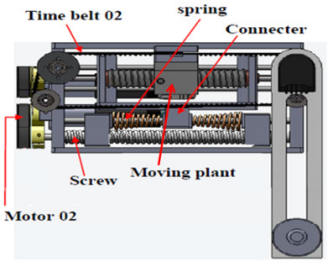

FIGURE 4: The Spring Absorb Forces from External Environment.

2.2 Modeling of APVSEA by Bond Graph Method

In order to simplify modeling of the APVSEA system, we treat the model as a human pushing a *spring-mass-damper system* in a car without ground contact friction, as shown in Figure 5. Because the human force is internal to the car, it cannot move the car forward. In other words,

the human's absolute position can be changed by car moving, but the human cannot drive the car forward.

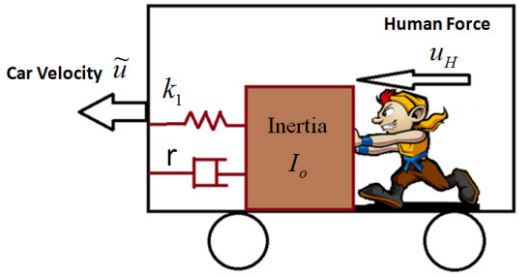

FIGURE 5: The APVSEA system can be briefly represented as human pushing a mass-damper-spring system in a car.

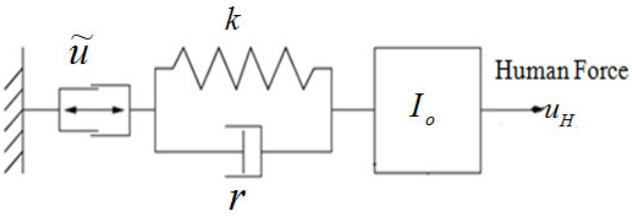

FIGURE 6: The Simplified APVSEA Model.

Figure 6 shows a simplified APVSEA model, where $\tilde{u}$ is the control input from motor 01 and u_H is the external force applied by the user. The inertia, spring stiffness and damping ratio are denoted by I_o, k, and r.

Based on the APVSEA model, the system model is converted into bond graph, as shown in Figure 7. The source-sensor element is represented as SS. Se and Sf are defined as the sensor, the effort and the flow sources, respectively. Bond graph elements I, C, R mean inertia, spring and damper in mechanical domain, respectively. The bond graph junction elements are denoted as 1 and 0 (black number). The bond numbers are also defined as red words in Figure 7. There are two TF elements. α and β represent the output link's rotational velocity $\dot{\theta}_o$ and the motor rotational velocity $\dot{\theta}_m$ converting into a horizontal movement, respectively. $\hat{u}$ represents the torque summation which is caused by gravity and human applied force on the output link. The velocity of spring is denoted as $\dot{\tilde{x}}$

.

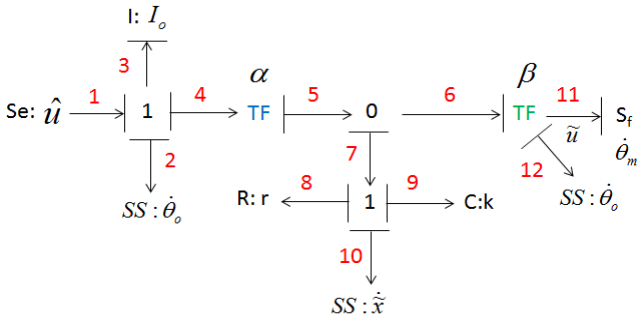

FIGURE 7: The APVSEA Bond Graph Model.

3. ROBUST FAULT DETECTION AND ISOLATION STRATEGY

In practice, the system can be separated into two parts: the nominal part and the uncertain part. Although the nominal part of the system is easy to model, the uncertain part, which includes

noises, error nominal value and so on, is hard to profile accurately and affects the performance of FDI. Djeziri et al. An adaptive FDI approach [10] was proposed to obtain a dynamic threshold, but this approach still needs to manually set some parameters for modeling uncertainties, which requires the designer to adjust by trial and error. Although adaptive FDI can filter out most of the uncertainties and make dynamical changes to determine the upper and lower thresholds, noises still exist and cause errors in the FDI system.

This paper adopts the approach in [10] to filter out the uncertain parts, and also proposes a doubt index approach to strengthen the robustness of fault detection. In addition, we adopt bond graph to generate ARRs to detect faults in the system. Therefore, if failures occur, the RFDI system can select a suitable isolation strategy based on the fault component. The proposed RFDI structure is shown in Figure 8.

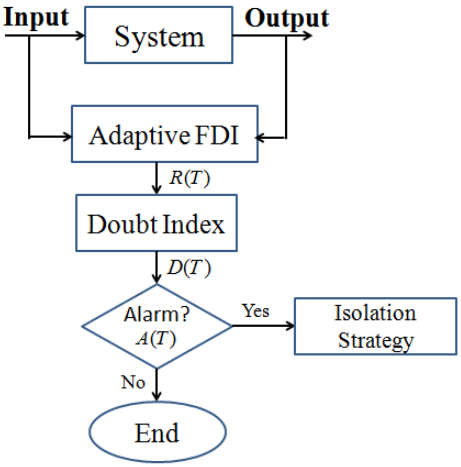

FIGURE 8: The RFDI Flow Chart.

3.1 Doubt Index

Doubt index is like an agent who can judge whether the system has faults based on his experience, like the "process manager," who knows each product's quality and determines whether the online process of the machine tool is operating normally. The process manager knows there are inevitably some defective products, but he also knows occasional defective products can be allowed in a long-term production process. But the manager will start to doubt the production line's functionality, if defective products appear more regularly, the doubt index will increase in his mind until the maximal tolerance is reached. Then he will announce an error alarm.

Let the i-th residual value r_i be the value of the i-th ARR equation, which is the nominal model obtained from physical laws. But in practice, a system does not perfectly follow the nominal model because of unknown parameters, such as noises, input variations, and transient periods. Suppose there are n residual equations in the system. Define

$$\tilde{r} = [r_1, r_2, \cdots r_n] \tag{1}$$

Then, the adaptive decision $\theta(\tilde{r})$ used to dynamically adjust the threshold δ_i can be defined as

$$C = [\theta(\tilde{r})] = [c_1, c_2, c_3 \cdots c_n] \tag{2}$$

$$c_i = \begin{cases} 1, \text{ if } |r_i| > \delta_i \\ 0, \text{ otherwise} \end{cases} \tag{3}$$

where δ_i is the threshold of c_i. When c_i equals to 1, an error is occurring in the corresponding ARR equation. The corresponding ARR equation is normal when c_i equals to 0.

In the past, some machine tools set δ_i as a constant, because the product processes are known and stationary. The designer can tune constant threshold values based on each machine tool's working situation. Unfortunately, this does not work for the robot system, because a robot's inputs are often dynamic, and therefore each input to actuator will require a different threshold. In other words, setting a constant threshold is not practical for robot systems.

In this paper, we consider uncertainties in each ARR equation for dynamically tuning thresholds δ_i [10]. Figure 8 shows the flow chart of the combination of adaptive FDI and doubt index. As mentioned above, it is not easy to adaptively tune all parameters, so sometimes a false alarm would sound due to bad tuning. Observing $R(T)$ the output of adaptive FDI, for example, we can regard that a fault occurs if $R(T)$ equals to 1 constantly for more than the setting time (the time setting which is tuned in terms of each case by the designer) is. On the other hand, when $R(T)$ behaviors like an impulse and are discontinuous, that is the error alarm fires for no more than the setting time, those should be filtered out by doubt index. Therefore, a doubt index $D(T)$ can be designed to determine whether a fault actually occurs as :

$$A(T) = D\left[R(T)\right] \tag{4}$$

where $A(T)$ is an alarm index, which equals to 1 if the system has fault, and 0 otherwise. $D(\cdot)$ is the doubt index, and $R(T)$ is the output of adaptive FDI. T denotes the integer time index of each input data.

The designer can develop the doubt index as the way a human doubts something. For example, if an adaptive FDI determines the system has fault error in the system, $R(T)$ will be 1. In the past, the system alarm is sounded due to $R(T)$ equaling to 1. But if the system adopts the doubt index method, it can judge whether the adaptive FDI has a false alarm. If $R(T+1)$ is 0, the doubt index can treat $R(T)$ as a false alarm and decrease the value of doubt index. However, if $R(T+1)$ equals to 1, the doubt index will be increased until it reaches a set limit. Then, $A(T)$ will announce the alarm signal.

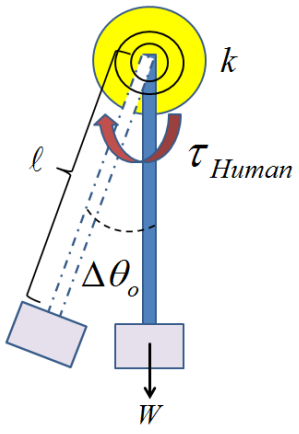

FIGURE 9: Human applies a small torque to the output link and causes slight rotation.

3.2 Zero Gravity Control

ZGC is an isolation strategy, different from an abrupt emergency stop. In this paper, we adopt ZGC because it can compensate for the mechanism's weight so that the user can apply a smaller force to drive the output link. Such system is especially useful for motor-impaired people;

otherwise, if the isolation strategy is only an emergency break, the entire weight of the robot would collapse on the user.

APVSEA has an intrinsic measure for torque sensing, as shown in Figure 9. The elastic property that the output link is rotated by $\Delta\theta_O$ when small forces are applied to the output link can be given as

$$W\ell \sin \Delta\theta_o = k \cdot \Delta x \quad \textbf{(5)}$$

Equation (5) can be used to compensate for the gravity torque, where W are the total weight of the object and output link. ℓ is the centroid length, and $\Delta\theta_o$ is a rotation caused by τ_{Human}. Since APVSEA is an elastic mechanism, k denotes the spring stiffness, and Δx corresponds to the rotational displacement of the equivalent spring. Equation (5) can be explained as human applying torque to APVSEA to generate the rotational displacement $\Delta\theta_o$. Therefore, we can translate the APVSEA's spring displacement reference input Δx from (5) to equation (6)

$$\Delta x = \frac{W\ell \sin \Delta\theta_o}{k} \quad \textbf{(6)}$$

Because the potentiometer behind the linear spring in APVSEA can measure the displacement of spring $\tilde{x}$, a proportional-integral-derivative (PID) controller is employed to track the reference input Δx . The ZGC control structure is shown in Figure 10.

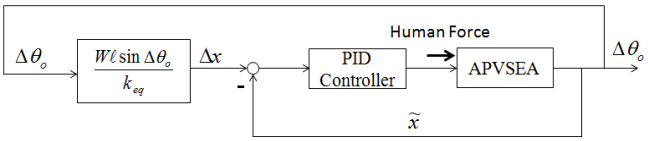

FIGURE 10: ZGC Controller Structure.

ROBUST FDI DESIGN FOR APVSEA

4.1 The Effect of APVSEA Element Broken

Before we develop the RFDI mechanism, it is necessary to understand what happens when an element of APVSEA is broken. Some machine tools have a fault detection function. If the machine tool fails, an emergency stop is traditionally considered as the best approach. But in the case of HRI (human robot interaction), human injury is possible due to the emergency stop. Therefore, in order to propose suitable isolation strategies, it is necessary to understand the injury effect of each broken component on the user.

The encoder is an important feedback signal for the control loop. If the encoder is broken, it will make the whole system out of control. In this paper, we are concerned with the encoders of motor 01 and the output link. If either of them fails, the control systems would diverge, dangerous if the actuator is used in exoskeletons or HRI robots. The potentiometer, used to measure the displacement of the spring to estimate force, is an important force information for the force control. Together with the encoder, the potentiometer affects the control system when it is damaged.

The cable and the timing belts are used to transmit energy in APVSEA. In other words, APVSEA loses its motor power when either of them is broken. In the case of exoskeletons or serial robots, because all actuators cascade, human or other actuators of the robot arm have to offer extra power to support the broken actuator and may injure the user.

Also, unexpected external force applying to the output link might be generated. For example, an exoskeleton robot is attached to the human body, so the human rejects the robot when he or she feels uncomfortable. Another case is when an unexpected obstacle collides with the output link of the APVSEA. These two scenarios may be dangerous for humans.

In summary, the APVSEA has six components of concern: motor 01 encoder, output link encoder, potentiometer, cable, timing belt, and external unexpected force. This paper develops fault detection for these components and proposes strategies to avoid damage in HRI applications.

4.2 Inverse Model with Uncertainty Part

In order to obtain the inverse APVSEA system from the bond graph model shown in Figure 11, the definition of power lines is needed, which is represented as blue lines in Figure11. Changing each storage bond graph element passed through by the blue line becomes a bi-causal notation.

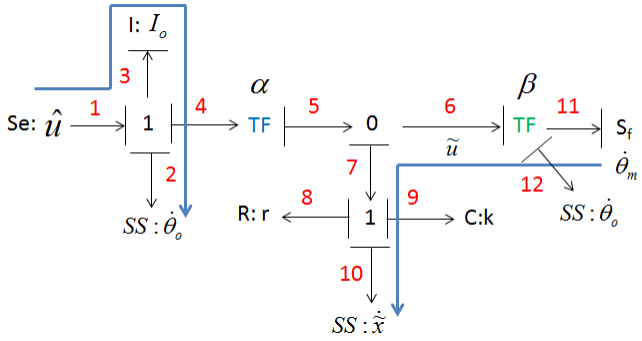

FIGURE 11: The Extend APVSEA Bond Graph.

To derive the inverse system, first, we define the uncertain elements of APVSEA. The uncertainty is caused by unknown parameters or external noises. The unknown parameters behind each bond graph element will be defined. Therefore, the inverse system of APVSEA associated with uncertain parts is given in Figure 12.

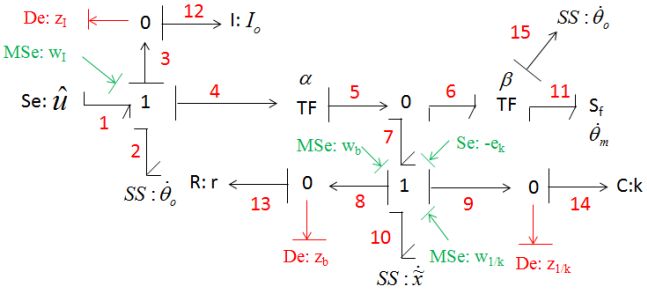

FIGURE 12: The extend APVSEA bond graph includes uncertain parts.

The red and green bonds represent the uncertainties, which had been defined in [10]. These equations are listed as:

$$w_b = -\frac{\Delta r}{r} z_b \tag{7}$$

$$w_{1/k} = \frac{\Delta k}{k + \Delta k} z_{1/k} \tag{8}$$

$$w_I = -\frac{\Delta I_o}{I} z_I \tag{9}$$

where $z_b = b\dot{x}$, $z_{1/k} = kx$, and $z_I = I_o\ddot{\theta}_o$. Δr, Δk and ΔI_o are uncertain parameters. De and MSe mean detect effort and module effort source.

4.3 ARR Equations and Fault Signature Matrix

First, we need to know how many ARR equations are behind the system. From Figure 11, there are 11 structural equations, three bond graph elements, three sensors, two actuators, and 16 unknown variables. Thus, the number of ARR equation is

$$\text{Number of ARR} = (11+3+3+2)-16 = 3 \tag{10}$$

These two equations can be obtained by the inverse bond graph shown in Figure 12 as:

$$\text{ARR1: } r_1 = \hat{u} - I_o\ddot{\theta}_o - \alpha b\dot{x} - \alpha kx + U_1 \tag{11}$$

$$\text{ARR2 : } r_2 = b\left(\beta\dot{\theta}_m - \alpha\dot{\theta}_o + \dot{x}\right) + k\left(\beta\theta_m - \theta_o + x\right) + U_2 \tag{12}$$

where U1 and U2 are uncertain parts. The total torque $\hat{u}$ that applies to the output link is very hard to accurately measure. Fortunately, the APVSEA is a serial elastic actuator, and therefore $\hat{u}$ can be measured by the potentiometer. The corresponding equations are

$$U_1 = \alpha\left(w_b + w_{1/k} - e_k\right) + w_I \tag{13}$$

$$U_2 = w_b + w_{1/k} - e_k \tag{14}$$

$$\hat{u} = \alpha kx \tag{15}$$

In equation (14), there is an initial condition e_k. We set e_k as zero in this case. But the two ARR equations above cannot completely detect each concerned component. Because all concerned components cannot be isolated by equations (11) and (12). A new ARR equation for the APVSEA needs to be added.

The output link is driven by a motor through the timing belt and ball-screw. In other words, there is a constant transmission ratio between the motor and the output link. This relationship can be used to obtain the third ARR equation.

$$\text{ARR3: } r_3 = \left|\theta_m\right| - \gamma\left|\theta_o\right| \tag{16}$$

where γ is the transmission ratio between the actuator rotation angle θ_m and the output link rotation angle θ_o. Although no uncertain parameter exists in ARR3, an error might be generated due to elastic vibration. Therefore, setting a suitable threshold is still needed as

$$\begin{cases} |r_3| < s, \text{ no fault} \\ |r_3| \geq s, \text{ fault} \end{cases} \tag{17}$$

where s is the ARR3 threshold value.

Fault signature matrix (FSM) is a fault index that can be used to isolate a fault component. Each ARR equation has the corresponding effect components, and identifying the effect components from each ARR equation is important for constructing the FSM. The FSM of the APVSEA is shown in Table I. If the residual equation is related to component faults, the matrix index is 1, otherwise, it is 0. M_b denotes the monitor ability of the component fault in the corresponding row. We set the index to 1 when the corresponding component is detected; otherwise it is 0. This means that if the fault signature of the element is not null, then $M_b = 1$. Similarly, I_b means there is an isolation ability in the component fault. If no residual row depends on each other, the I_b index is 1; otherwise it is 0. This means the FSM can isolate fault components.

Component Name	A_1	A_2	A_3	M_b	I_b
External Unexpected Force	1	0	0	1	1
Output Link Encoder	1	1	1	1	1
Potentiometer	1	1	0	1	1
Cable/Timing belt	0	1	0	1	1
Motor01 Encoder	0	1	1	1	1

TABLE 1: FSM of APVSEA.

Table I shows five sensitive components using three residuals equations. $\mathrm{A_i}$ represents the i-th ARR equation which has been processed by doubt index. Note that all the elements in columns M_b, and I_b are 1. This means that the FSM in Table I can monitor and isolate all the concerned components.

4.4 Doubt Index Design

The adaptive FDI can filter out most of false alarms, but some of them still inevitably pass. Filtering out misdetection is the goal at this stage. The false alarm time is set not to exceed 0.1 seconds. The false alarm time depends on each different case. The output of the adaptive ARRs is doubt index input, and a false alarm looks like a sudden impulse with duration no longer than 0.1 seconds. This means if the alarm time is longer than 0.1 seconds continuously, the FDI system can judge whether there is a component fault. Hence, the doubt index is designed as

$$D(T+1) = R(T) \times \left[1 + D(\mathrm{T})\right] \tag{18}$$

Equation (18) can be used to eliminate false alarms. This equation is recursive. When the adaptive FDI announces a fault, equation (18) will increase doubt index value. In this paper, if the doubt index is over 100 (i.e. the fault announcement duration is more than 0.1 seconds), the system will judge that there is a component fault occurring.

4.5 Fault Tolerance Control

In the above sections, we discuss why a pure emergency stop could be dangerous for human, but such danger can be avoided with FTC, which switches the system's controller to keep humans safe. In this paper, there are two isolation strategies: emergency stop and ZGC. The FTC system in APVSEA is shown in Figure 13, in which $\mathrm{y_{ref}}$ and $\mathrm{y'_{ref}}$ are the control inputs for nominal controller and ZGC, respectively.

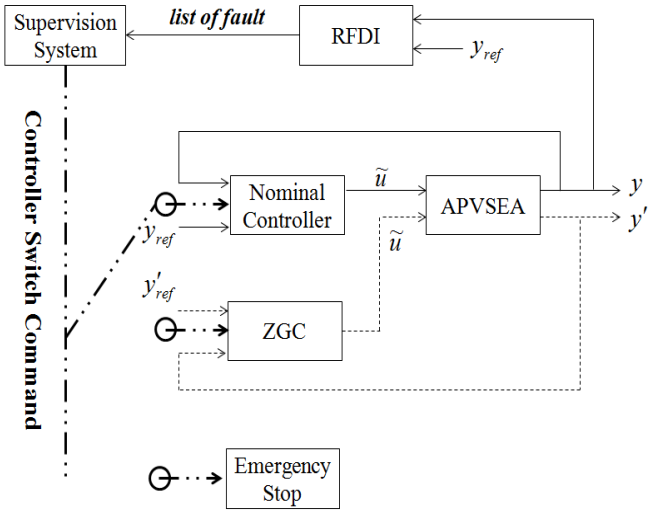

FIGURE 13: Fault Tolerance Controller Structure.

The supervision system, which is used to decide which controller to activate based on a list of faults from the RFDI, is the key for the switching between controllers. Before constructing a supervision system, it is necessary to know how a fault component affects the system, as mentioned earlier. Based on these effects, the switching strategies of the supervision system are designed as in Table II. In general, ZGC is preferred. An emergency stop will only be used, when either the belt or the cable breaks. Because the timing belt and the cable are power transmission units, when they fail, the system cannot be driven by any actuator or power source. Therefore, stopping the system is the only choice in this case.

Fault Component	Supervision System
Motor 01 encoder	Zero Gravity Control
Output link encoder	
Potentiometer	
External unexpected force	
Timing belt	Emergency Stop
Cable	

TABLE 2: Isolation Strategies.

4.6 Zero Gravity Controller Design

Equation (6) above is the key formula for ZGC, which requires the measurements of the output link's rotation angle $\Delta\theta_o$ and the spring's elongation $\tilde{x}$. But, equation (6) does not hold if the output link's encoder or potentiometer is broken. In order to realize the ZGC isolation strategies, which are shown in Table II, the ZGC equation (6) has to be modified to consider the fault of encoder or potentiometer.

The first situation is when motor 01 encoder fails or when unexpected external force occurs. These two faults do not influence equation (6) operation, so ZGC can be realized using equation (6) when motor 01 encoder fails.

The second case is when the output link's encoder fails. In order to estimate the rotation of the output link θ_o, it should be calculated by another sensor. If motor 01's encoder and potentiometer

are working normally, those can be used to estimate the rotation angle of the output link. The relationship among motor 01's encoder, potentiometer, and the output link's encoder can be shown by Figure 12. The displacement of the spring, which relates to the rotation angles of the output link and motor 01, is

$$f_9 = f_5 - f_6 \tag{19}$$

where f_i means the i-th flow bond from Figure12. In other words,

$$\tilde{x} = x_H\left(\theta_o\right) - x_M\left(\theta_M\right) \tag{20}$$

where $x_H(\theta_o)$ and $x_M(\theta_M)$ mean the horizontal displacement relationships between the output link angle and motor rotation angle. Therefore, equation (20) can be used to estimate the output link's rotation angle when the output link's encoder is broken. This leads to an alternate ZGC equation (6)

$$\Delta x = \frac{W\ell \sin\left(\tilde{x} + x_M\left(\theta_M\right)\right)}{k} \tag{21}$$

The third case is when the potentiometer fails. In the ZGC control structure shown in Figure10, the potentiometer is used to generate a feedback signal of the displacement of the moving plant. Therefore, equation (20) can also be used to replace the original feedback potentiometer signal $\tilde{x}$.

4. EXPERIMENTS

In this section, three experiment results are presented. Part 5.1 is the experimental result of RFDI. The comparison among constant threshold, adaptive threshold and adaptive threshold combined with doubt index will be presented. The realization of ZGC approach in the APVSEA is demonstrated in Part 5.2. The effect of RFDI will be shown in Part 5.3 and Appendix. RFDI not only detects component fault but also isolates it. Switching the system's controller to ZGC or emergency stop based on each component fault situation is demonstrated.

5.1 Combination of Adaptive FDI and Doubt Index

In order to illustrate the differences between constant thresholds, adaptive thresholds, and the adaptive thresholds combined with doubt index, Figure 14 shows the ARR1 signal and each approach's alarm index. If the index value is equal to zero, this means there is no faults occurring. On the contrary, if the FDI system determines that there is a fault occurring in the APVSEA, the alarm index value displays 1. This experiment was executed in the situation where the APVSEA suffered unexpected external force interact with the user. Figure 14(a) shows the ARR1 signal that is affected by an unexpected external force in the fault area. The top two diagrams in Figure 14(b) displays constant and adaptive thresholds. The third diagram of Figure 14(b) represents the experimental result of the adaptive threshold combined with doubt index.

According to the first diagram of Figure 14(b), the constant threshold demonstrates that it is not easy to determine whether a fault occurring in the system is due to noises or uncertain parameters. Therefore, there are some false alarms in no fault areas. An adaptive threshold approach can adjust its thresholds depending on noises or uncertain parameters. Thus, its fault detection performance is better than the approach using constant thresholds. But, there are still some false alarms, which are similar to impulses.

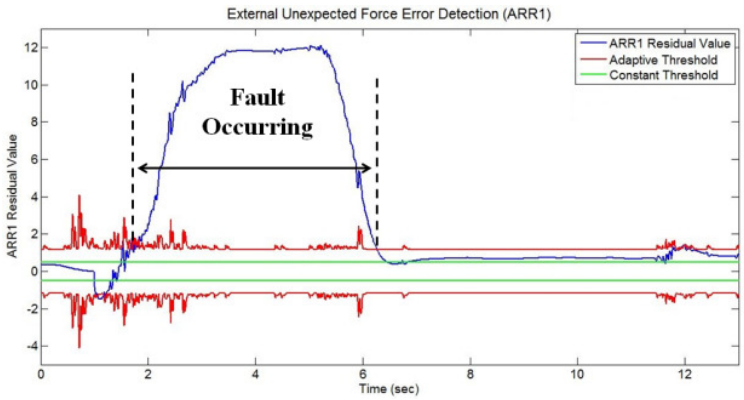

FIGURE14(a): The ARR of External Unexpected Force Fault.

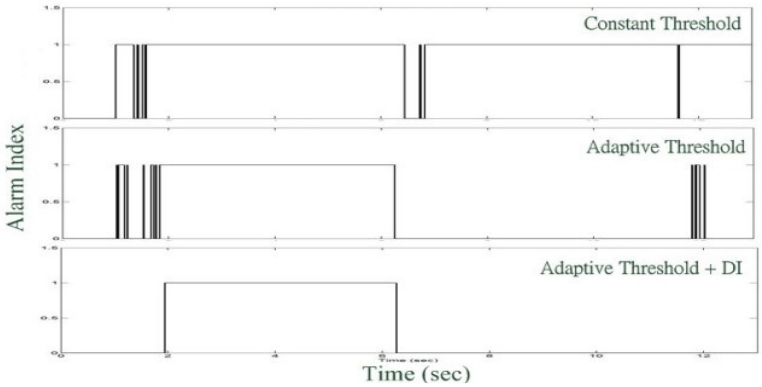

FIGURE 14(b): The Alarm Index of Each Approach.

The adaptive threshold approach combined with doubt index can eliminate those impulses and show only the true fault area, as shown in the third diagram of Figure 14(b). But, this approach still has the problem of delayed fault determination, which depends on the design of doubt index parameter. In this experiment, we designed the doubt index parameter that generates a 0.1 seconds delay in determination.

5.2 The Experiment of Zero Gravity Control

The ZGC's experimental results are shown in Figure 15. The results can be separated into two stages. Stage 1 shows when the motor of the APVSEA was off while the user swung the output link back and forth, causing a reaction torque on the APVSEA. Stage 2 shows the ZGC's experimental results. There are angle difference between the motor angle and the output link's angle. If the output link's angle is bigger, the angle difference is larger. Therefore, the APVSEA generates torque to compensate for gravity torque due to the different angle between the output link's angle and motor01. In Figure 15, the horizontal lines of the output link's angle represents that the user released operating force, and the link was held at the same position by ZGC. It is clear that holding output link needs larger gravity torque compensation if the output link angle is bigger.

Since ZGC compensated for the gravity torque of the output link, it could make sure that the user operated safely. In addition, because the user did not apply extra forces to hold the robot's weight, the user can move the robot easily.

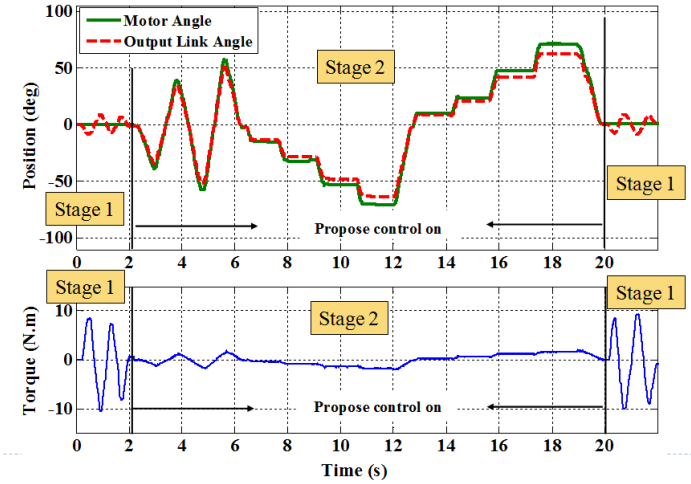

FIGURE 15: Zero Gravity Control in APVSEA.

5.3 Robust Fault Detection and Isolation

RFDI not only detects fault components but also selects the suitable controller for human safety when the system has any component fault. This paper proposes FTC switching strategies in Table II and the rule for fault detection in Table I. This part of experimental result presents RFDI's fault detection and isolation ability. The abilities of supervision and controller switching are also shown at this part. There are five fault situations and isolation strategies which had been listed in Table II.

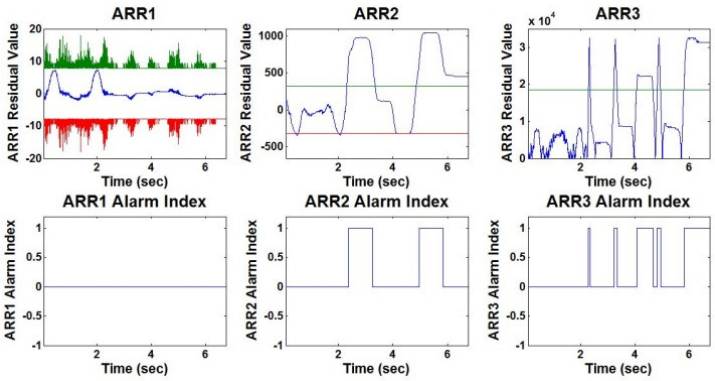

FIGURE 16: Motor 01 Encoder Fault at 2.3 Seconds.

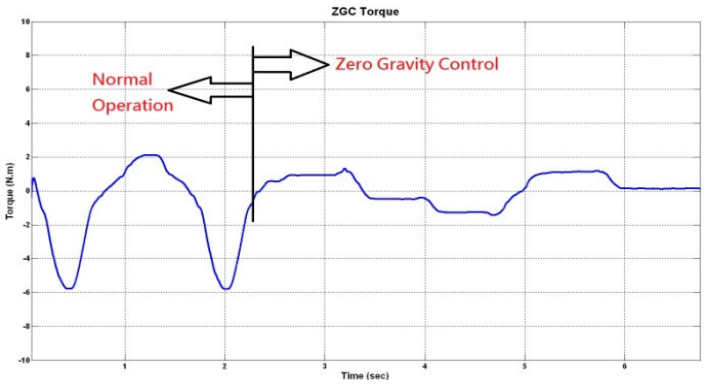

FIGURE 17: Switch Controller to ZGC when Motor 01 Encoder is Fault.

The settings of the following experiments were the same. The input of the output link of APVSEA followed a sine wave. Then, various fault situations were created by the operator. For example, we unplugged the sensor (encoder, potentiometer), cut off the timing belt or generated unexpected force deliberately by human randomly, in order to verify whether the RFDI can detect the fault and switch the controller to keep human safe.

The scenario of motor encoder fault is presented in Figure 16 and Figure 17, other experiment results will be shown in Appendix. In Figure 16, the motor encoder was unplugged at 2.3 seconds. The green and red curves of Figure 16 are dynamic threshold which were generated by adaptive FDI. The blue curve which presents at the upper plot of Figure 14 represents residual value of each ARR equation. ARR alarm index is shown in the lower plot of Figure 16. It is worth mentioning that the alarm index was processed using doubt index. Therefore, even there are some residual values over dynamic threshold which is generated by adaptive FDI, they were filtered out.

RFDI can determine which component is suffering from fault situation based on Table I. The lower plot of Figure 16 indicates there is a component fail at 2.3 seconds. At 2.3 seconds, the ARR alarm indexes are

$$\left(A_1, A_2, A_3\right) = \left(0,1,1\right) \tag{22}$$

Mapping equation (22) to Table I can judge which component fails.

The system's controller is switched by FTC for ensuring human safety. Table II is FTC's decision criteria. There are two situations in Figure 17. Normal operation means the system has no fault and works normally. In this case, the component fails at 2.3 seconds. Therefore, FTC system switched the system's controller to ZGC at 2.3 seconds.

However, there are still some false alarms which occur after 2.3 seconds in ARR2 and ARR3. Those do not affect RFDI determination, because the system has been changed to ZGC. In other words, if the system's controller has been modified to the other control situation (ZGC or emergency stop), the fault detection function is disabled so that further alarm indexes will not affect the FTC.

In Appendix, Figure A.4 represents cable broken situation at 3.3 seconds. As mentioned earlier, if the cable or timing belt breaks, emergency stop will be the best approach for human safety. Therefore, the lower plot of A.4 is voltage signal, and the system's voltage is stopped at 3.3 seconds.

5. CONCLUSION

While robot interacts with humans, safely is the most important issue. However, because a robot is a complex machine, it is hard to guarantee that no key component of the robot will malfunction or suffer from unexpected external forces. This paper proposed a RFDI approach that includes the adaptive FDI, doubt index, and isolation strategies. The adaptive FDI can consider uncertain parts and adjust the detection thresholds to avoid false alarms, but this approach still generate false alarms because uncertain parameters setting. The doubt index approach is used to further eliminate those false alarms that escape from the adaptive FDI. Finally, with low cost, a ZGC without using expensive force sensor was implemented as an one of isolation strategies in the RFDI of APVSEA to make sure that the working environment is safe when the robot breaks. From the experimental results, the RFDI approach is useful for determining component faults in a system without raising false alarms, and isolation strategies, including an emergency stop and ZGC, can ensure the user's safety.

6. FUTURE WORK

In this paper, doubt index is designed using very simple method. It accumulates fault alarms when it's happening time is over than 0.1 seconds. The doubt index design in this paper will cause the RFDI decision time delay. Therefore, doubt index design can be smart using intelligent algorithm, so that can decrease the decision time.

7. REFERENCES

[1] R.J. Wang, H.P. Huang, "An Active-Passive Variable Stiffness Elastic Actuator for Safety Robot Systems," *IEEE/RSJ International Conference on Intelligent Robots and Systems (IROS)*, Taipei, pp. 3664-3669, Oct. 18-22, 2010.

[2] K. Medjaher, " A bond graph model-based fault detection and isolation," *Maintenance Modelling and Applications*, Chapter 6: Fault Diagnostics, pp. 503-512, 2011.

[3] K.A. Samantaray, O.B. Belkacem, "Bond Graph Model-based Quantitative FDI," *Model-based Process Supervision: A Bond Graph Approach*, pp. 177-228, 2008.

[4] I. Hwang, S. Kim, C.E. Seah, "A Survey of Fault Detection, Isolation, and Reconfiguration Methods," *IEEE Transactions on Control Systems Technology*, Vol. 18, No. 3, pp.636-653, 2010.

[5] K. Emami, B. Nener. V. Sreeram, H. Trink, T. Fernando, "A Fault Detection Technique for Dynamical Systems," *IEEE Conference on Industrial and Information Systems (ICIIS)*, Sri Lanka, pp. 201-206, Aug. 18-20, 2013.

[6] B. Pourbabaee, N. Meskin, K. Khorasani, "Sensor Fault Detection and Isolation using Multiple Robust Filters for Linear Systems with Time-Varying Parameter Uncertainty and Error Variance Constraints," *IEEE Conference on Control Applications (CCA)*, Juan Les Antibes, pp. 382-389, Oct. 8-10, 2014.

[7] V. Venkatasubramanian , R. Rengaswamy , K. Yin and S. N. Kavuri "A review of process fault detection and diagnosis part I: Quantitative model-based methods," *Computer and Chemical Engineering*, Vol. 27, pp.293 -311, 2003.

[8] V. Venkatasubramanian , R. Rengaswamy , K. Yin and S. N. Kavuri "A review of process fault detection and diagnosis part II: Qualitative models and search strategies," *Computer and Chemical Engineering*, Vol. 27, pp.313 -326, 2003.

[9] V. Venkatasubramanian , R. Rengaswamy , K. Yin and S. N. Kavuri "A review of process fault detection and diagnosis part III: Process history based methods," *Computer and Chemical Engineering*, Vol. 27, pp.327 -346, 2003.

[10] M.A. Djeziri, R. Merzouki B.O. Bunamama, D.T. Genevieve, "Robust Fault Diagnosis by Using Bond Graph Approach," *IEEE Transactions on Mechatronics*, Vol.12, No. 6, pp.599-611, 2007.

[11] W. Bouallegue, S.B. Bouabdallah, M. Tagina, "A new adaptive fuzzy FDI method for bond graph uncertain parameters systems," *IEEE International Conference on Electronics, Circuits and Systems (ICECS)*, Beirut, pp.643-648, Dec. 11-14, 2011.

[12] W. Bouallegue, S.B. Bouabdallah, M. Tagina, "Causal approaches and fuzzy logic in FDI of bond graph uncertain parameters systems," *International Conference on Communications, Computing and Control Applications (CCCA)*, Hammamet, pp.1-6, Mar. 3-5, 2011.

[13] R. Loureiro, R. Merzouki, B.O. Bouamama, "Bond Graph Model Based on Structural

Diagnosability and Recoverability Analysis: Application to Intelligent Autonomous Vehicles," *IEEE Transactions on Vehicular Technology*, Vol. 61, No. 3, pp. 986-997, 2012.

[14] R. Loureiro, S. Benmoussa, Y. Touati, R. Merzouki, B.O. Bouamama, " Integration of Fault Diagnosis and Fault-Tolerant Control for Health Monitoring of a Class of MIMO Intelligent Autonomous Vehicles," *IEEE Transactions on Vehicular Technology*, Vol. 63, No. 1, pp.30-39, 2014.

[15] Y. Touati, R. Merzouki, B.O. Bouamama, "Robust Diagnosis to Measurement Uncertainties using Bond Graph Approach: Application to Intelligent Autonomous Vehicle," *Mechatronics*, Vol.22, No.8, pp. 1148-1160, 2012.

[16] S. Benmoussa, B.O. Bouamama, R. Merzouki, "Bond Graph Approach for Plant Fault Detection and Isolation: Application to Intelligent Autonomous Vehicle," *IEEE Transactions on Automation Science and Engineering*, Vol.11, No.2, pp.585-593, 2014.

[17] M. Talebpur, M. Namvar, "Zero-Gravity Emulation of Satellites in present of Uncalibrated Sensors and Model Uncertainties," *IEEE Conference on Control Applications & Intelligent Control, Saint Petersburg*, pp.1063-1068, July 8-10, 2009.

[18] M. Geravand, F. Flacco, A.D. Luca, "Human-Robot Physical Interaction and Collaboration using an Industrial Robot with a Closed Control Architecture," *IEEE International Conference on Robotics and Automation*, Karlsruhe, Germany, pp. 4000-4007, May 6-10, 2013.

[19] A. Vick, D. Surdilovic, J. Kruger, "Safe Physical Human-Robot Interaction with Industrial Dual-Arm Robots," *Workshop on Robot Motion and Control (RoMoCo)*, Kuslin, pp. 264-269, July 3-5, 2013.

[20] G. Hirzinger, A. Albu-Schaffer, M. Hahnle, I. Schaefer, N. Sporer, "On a New Generation of Torque Controlled Light-Weight Robots," *IEEE International Conference on Robotics and Automation (ICRA)*, Seoul, Korea, Vol.4, pp. 3356-3363, 2001.

[21] G. Golo, van der Schaft, Arjan, P.C. Breedveld, B.M. Maschke., "Hamiltonian Formulation of Bond Graphs," *Nonlinear and Hybrid Systems in Automotive Control*, London, pp. 351-372, 2003.

APPENDIX

In this paper, five key components (external unexpected force, output link encoder, potentiometer, cable/timing belt and motor 01 encoder) need to be monitored. The experiment results when motor 01 encoder is broken has been shown in Figure 16 and Figure 17. This appendix will be demonstrated other fault situations. According to experiment results, each fault situation can be detected by RFDI and isolated to suitable controller by FTC for ensuring human safety.

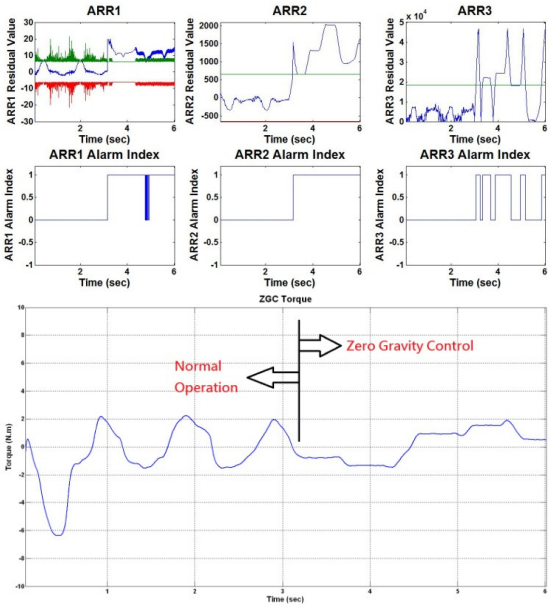

A.1: Output link encoder had fault at 3.2 seconds. The APVSEA had been turned to zero gravity control when the fault occurs.

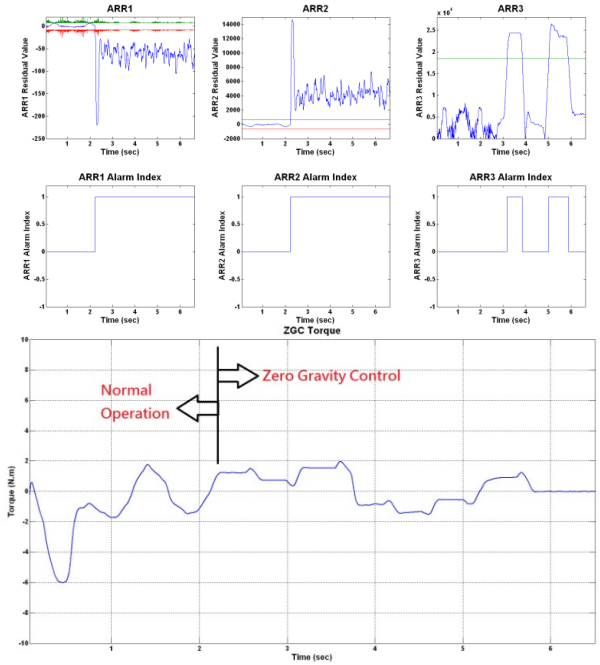

A.2: Potentiometer suffered from fault at 2.2 seconds. Even the potentiometer broke, zero gravity control can be implemented using motor and output link encoders.

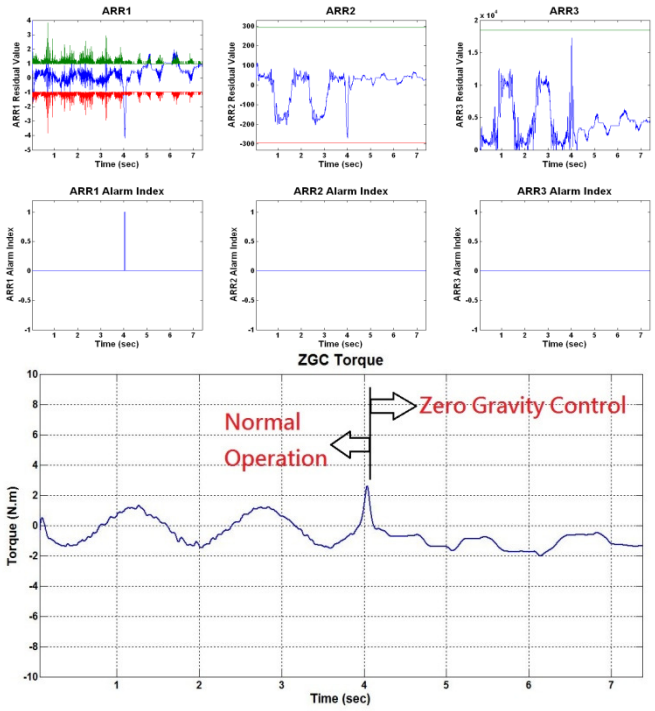

A.3: An unexpected force was applied at 4.1 seconds. Human can move the output link easily under zero gravity control to protect human safety.

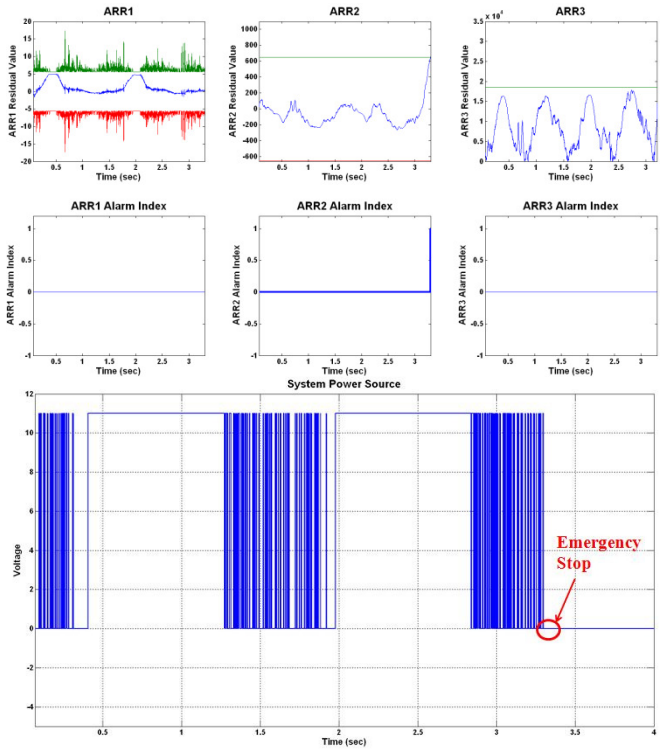

A.4: Cable is broken at 3.2 seconds, and the voltage is turned off due to emergency stop.